Environment International 140 (2020) 105754

Contents lists available at ScienceDirect

Environment International

journal homepage: www.elsevier.com/locate/envint

# Redox-induced mobilization of Ag, Sb, Sn, and Tl in the dissolved, colloidal and solid phase of a biochar-treated and un-treated mining soil

Jörg Rinklebe[a,b,*,1], Sabry M. Shaheen[a,c,d,1], Ali El-Naggar[e,f], Hailong Wang[g,h], Gijs Du Laing[i], Daniel S. Alessi[j], Yong Sik Ok[k,*]

[a] University of Wuppertal, School of Architecture and Civil Engineering, Institute of Foundation Engineering, Water- and Waste-Management, Laboratory of Soil- and Groundwater-Management, Pauluskirchstraße 7, 42285 Wuppertal, Germany
[b] Department of Environment, Energy and Geoinformatics, Sejong University, Seoul 05006, Republic of Korea
[c] King Abdulaziz University, Faculty of Meteorology, Environment, and Arid Land Agriculture, Department of Arid Land Agriculture, 21589 Jeddah, Saudi Arabia
[d] University of Kafrelsheikh, Faculty of Agriculture, Department of Soil and Water Sciences, 33516 Kafr El-Sheikh, Egypt
[e] State Key Laboratory of Subtropical Silviculture, Zhejiang A & F University, Hangzhou 311300, China
[f] Department of Soil Sciences, Faculty of Agriculture, Ain Shams University, Cairo 11241, Egypt
[g] Biochar Engineering Technology Research Center of Guangdong Province, School of Environment and Chemical Engineering, Foshan University, Foshan, Guangdong 528000, China
[h] Key Laboratory of Soil Contamination Bioremediation of Zhejiang Province, Zhejiang A & F University, Hangzhou, Zhejiang 311300, China
[i] Department of Green Chemistry and Technology, Ghent University, Ghent, Belgium
[j] Department of Earth and Atmospheric Sciences, University of Alberta, Edmonton, Alberta T6G 2E3, Canada
[k] Korea Biochar Research Center, O-Jeong Eco-Resilience Institute (OJERI) & Division of Environmental Science and Ecological Engineering, Korea University, Seoul 02841, Republic of Korea

ARTICLE INFO

*Keywords:*
Emerging contaminants
Release dynamics
Redox cycles
Charcoal
Rice paddy

ABSTRACT

The aim of this work was to study the redox-induced mobilization of Ag, Sb, Sn, and Tl in the dissolved, colloidal, and sediment phase of a mining soil treated and untreated with biochar as affected by the redox potential ($E_H$) -dependent changes of soil pH, dissolved organic carbon, Fe, Mn and S. The experiment was conducted stepwise at two $E_H$ cycles (+200 mV → -30 mV → +333 mV → 0 mV) using biogeochemical microcosm. Silver was abundant in the colloidal fraction in both cycles, indicating that Ag might be associated with colloids under different redox conditions. Antimony, Sn and Tl were abundant in the colloidal fraction in the first cycle and in the dissolved fraction in the second cycle, which indicates that they are retained by colloids under oxic acidic conditions and released under reducing alkaline conditions. Release of dissolved Sb, Sn, and Tl was governed positively by pH, Fe, S, and dissolved aromatic compounds. Biochar mitigated Ag release, but promoted Sb, Sn, and Tl mobilization, which might be due to the wider range of $E_H$ (-12 to +333) and pH (4.9–8.1) in the biochar treated soil than the un-treated soil ($E_H$ = -30 to +218; pH = 5.9–8.6). Also, the biochar surface functional groups may act as electron donors for the Sb, Sn, and Tl reduction reactions, and thus biochar may play an important role in reducing $Tl^{3+}$ to $Tl^{+}$, $Sb^{5+}$ to $Sb^{3+}$, and $Sn^{4+}$ to $Sn^{2+}$, which increase their solubility under reducing conditions as compared to oxic conditions. Thallium and Sb exhibit higher potential mobility in the solid phase than Sn and Ag. Biochar increased the potential mobility of Sb, Sn, and Tl under oxic acidic conditions. The results improve our understanding of the redox-driven mobilization of these contaminants in soils.

## 1. Introduction

Soil contamination by potentially toxic elements (PTEs) is globally of serious concern due to high risks to human and ecosystem health (Antoniadis et al., 2017; Rinklebe et al., 2019). Antimony (Sb), silver (Ag), tin (Sn), and thallium (Tl) are considered as emerging contaminants and toxic for human, animals, microorganisms and plants. For example, the toxicity of Tl is higher compared to Hg, Cd and Pb (Eqani et al., 2018). Antimony has been considered as a priority pollutant by the United States Environmental Protection Agency and by the European Union (Eqani et al., 2018; Al and Viraraghavan, 2005). These elements are redox-sensitive; therefore, their mobilization in

* Corresponding authors.
*E-mail addresses:* rinklebe@uni-wuppertal.de (J. Rinklebe), yongsikok@korea.ac.kr (Y. Sik Ok).
[1] These authors contributed equally to this work and should be considered first authors.

https://doi.org/10.1016/j.envint.2020.105754
Received 3 December 2019; Received in revised form 16 April 2020; Accepted 19 April 2020
Available online 01 May 2020

natural systems is largely controlled by redox potential ($E_H$) (Couture et al., 2015; Nakamaru and Altansuvd, 2014). Redox-induced release of dissolved concentrations of PTEs including Ag, Sb, Sn, and Tl in wetland soils, waterlogged sediments, and rice paddy soils is of increasing interest and has broader implications, due to the high potential risks to human health (Rinklebe et al., 2016a, b, 2017, 2019). For example, the redox-induced release of these emerging pollutants may cause an increase leaching to the ground water and thus may increase their transfer from soils to plant and food chain. In particular, Tl and Sb are responsible for many accidental, occupational, deliberate, and therapeutic poisonings (Al and Viraraghavan, 2005). Therefore, the fascinating chemistry and high toxicity potential of Sb and Tl and their compounds lead to the large scientific interest and high relevance for environmental and human health.

However, little is known about the redox-induced release of Ag and Sn, while few studies detail the release mechanisms of Sb (e.g., Hockmann et al., 2014; Han et al., 2018; Frohne et al., 2011) and Tl (e.g., Antić et al., 2017; Jia et al., 2018) in flooded soils. Nevertheless, those studies focused on the dissolved fractions of Sb and Tl while the concentrations of those elements in the colloidal fraction were not measured. Because there are large differences in toxicity among the different forms of Sb, Sn, and Tl (e.g., $Tl^{3+}$ is much more toxic than $Tl^{+}$ (Jia et al., 2018; Ralph and Twiss, 2002), a thorough understanding of the redox transformations of these elements and of their redox-dependent fate in soils is required in order to evaluate the potential associated risks. Unlike with some of other PTEs found in terrestrial environments, information about what controls the redox chemistry of Ag, Sb, Sn, and Tl in soils remains scarce (Jia et al., 2018; Al-Najar et al., 2005).

Biochar (BC) can be used to remediate soils contaminated with PTEs (Palansooriya et al., 2020); however, biochar application to contaminated soils can cause contradictory effects on elemental mobilization depending on the soil redox conditions (Yuan et al., 2017). Functional groups in biochar may contribute to its redox characteristics (Yuan et al., 2017; Klüpfel et al., 2014). The dissolved organic matter extracted from biochar can act as both electron donor and acceptor, reducing and oxidizing the elements (Yuan et al., 2017; Dong et al 2014). Also, the pyrolysis temperature of biochar affects significantly its redox characteristics and the redox-meditated interactions between biochar and PTEs in soils (Awad et al., 2018; Chen et al., 2018). Only few researchers (e.g. Rinklebe et al., 2016a; Beiyuan et al., 2017) addressed the effects of biochar amendment on the (im)mobilization of PTEs under dynamic redox conditions. However, these studies were dedicated solely to the fate of dissolved concentrations of PTEs; the colloidal fraction was not investigated, and the emerging contaminants Ag, Sb, Sn, and Tl were not studied.

Colloids are operationally defined as particles between 2 and 10 μm in diameter (e.g., de Jonge et al., 2004), and include layer silicates, sesquioxides (Fe- and Al-oxyhydroxides), organic macromolecules, and bacteria, and viruses. Mobilization of soil colloids has attracted much research attention from agro-environmental point of view, because of colloids' potential to facilitate transport of sorbed contaminants and nutrients. Although effect of colloids on the sorption of trace elements has been reported (Shaheen et al., 2013), its impact on redox- mobilization of emerging contaminates such as Ag, Sb, Sn, and Tl is not studied yet. Our previous studies (El-Naggar et al., 2018; El-Naggar et al., 2019) focused on other elements such as As, Cd, Cr, Cu, Mo, Se, and Zn. Thus, to our best knowledge, the redox-induced release of Ag, Sb, Sn, and Tl, in particular with respect to their concentrations in three phases of soil (the dissolved, colloidal, and the solid-phase) as affected by application of biochar, has never been tested. A proper understanding of biogeochemistry of Ag, Sb, Sn, and Tl in soils is very limited particularly under dynamic reducing-oxidizing conditions. Therefore, detailed knowledge about the redox-behavior of Ag, Sb, Sn, and Tl in soils is required to understand their mobilization processes and enable a more accurate prediction of their release into waters in response to changing redox conditions. It is also essential to understand the redox-driven mobilization of Ag, Sb, Sn, and Tl in soil so that their potential hazard can be better predicted.

We hypothesize that dynamic redox cycles in soil may (im)mobilize the redox-sensitive contaminants Ag, Sb, Sn, and Tl and redistribute them among the dissolved and colloidal fractions, due to changes in $E_H$ values, and/or the $E_H$–dependent changes of governing factors such as soil pH, dissolved aliphatic and aromatic compounds of organic carbon and the chemistry of iron (Fe) and manganese (Mn) (hydr)oxides, sulfur (S), and chloride ($Cl^-$). To support our hypothesis, we assume that the oscillations from oxidizing to reducing conditions and vice versa in the soil govern the release of Ag, Sb, Sn, and Tl and their solubility in a mining wetland soil. We also hypothesize that application of biochar would increase the capacity of a soil to accept and/or donate electrons by controlling electron transfer reactions, and thus lead to a wider range of $E_H$ in the soil slurry (Awad et al., 2018), which in turn may affect the associated governing factors (soil pH, dissolved organic carbon (DOC), Fe, Mn, and S) and, consequently, the mobilization of Ag, Sb, Sn, and Tl and their distribution in the dissolved and colloidal fractions as compared to the untreated soil.

Mining soils are distributed world-wide and are often contaminated by PTEs. Large areas of mining soils can be flooded periodically and cultivated by rice. In our study, the soil was collected from a mining area at Hubei province in China. Hubei is located in the agricultural transition zone between the wheat-growing North and the rice-growing South; it is one of China's leading rice-producing provinces. The average annual rainfall in Hubei Province is between 800 and 1600 mm. This soil might be flooded either during rice cultivation season or as a result of the heavy rains. Therefore, the scientific background of our study is to investigate the redox-induced mobilization of toxic elements in the soil when it will be flooded. Within this context we hypothesize that the periodic inundation of the soil may affect the release dynamics of Ag, Sb, Sn, and Tl due to the changes of $E_H$/pH-values and the above mentioned controlling factors.

To verify our hypotheses, we quantified the impact of pre-defined redox conditions on the release dynamics of Ag, Sb, Sn, and Tl in the dissolved and colloidal fractions and on their potential mobility in the solid-phase of a mining soil as affected by addition of rice hull biochar. We also determined the associations between the concentrations of Ag, Sb, Sn, and Tl and controlling factors ($E_H$, pH, DOC, Fe, Mn, S, and $Cl^-$) and identified the complex cause-and-effect interrelationships using factor analysis.

To the best of our knowledge, this is the first work which studies systematically the impacts of redox potential ($E_H$) cycles, biochar, and the $E_H$-dependent changes of soil pH, dissolved organic carbon, Fe, Mn, S, $Cl^-$, on the dissolved and colloidal concentrations of the emerging contaminates Ag, Sb, Sn, and Tl and their potential mobility in a mining soil. We used a combination of geochemical and spectroscopic approaches to verify our previous hypotheses and ultimately provide an understanding of the fundamental mechanisms that control the redox-mediated interactions between Ag, Sb, Sn, and Tl with biochar. It also elucidate the biogeochemical processes control the release dynamics and distribution of Ag, Sb, Sn, and Tl among the dissolved and colloidal fraction, as well as their potential mobility in the solid phase.

## 2. Materials and methods

### 2.1. Sampling, preparation, and characterization of the studied soil and biochar

A composite surface soil sample (0–20 cm) was collected from an ore processing site in Hubei Province, China. Information on the sampling site is provided in Li et al. (2016), and El-Naggar et al.(2018). The soil samples were air dried and sieved through a 2-mm sieve and characterized according to Blume et al. (2011) X-ray fluorescence spectroscopy (XRF, ZSX Primus II, Japan) was used to assess the elemental composition of the inorganic compounds in the soil. Basic

characteristics of the soil are provided in the supporting information (Appendix A in Table S1).

The biochar was produced from rice hull by DAEWON GSI Company, Korea. Awad et al. (2018) reported that biochar produced at a high pyrolysis temperature (e.g., 550 °C) may cause larger redox alterations in soil slurry compared to one produced at a lower temperature (e.g., 300 °C). Accordingly, we chose a biochar produced with a high pyrolysis temperature (500 °C). Following pyrolysis, the biochar was prepared for characterization and soil mixing experiments by grinding in a mortar and passing through a 2-mm sieve. The product was characterized for ash, carbon, moisture, and volatile matter content using a muffle furnace (MF21GS, JEIO TECH, Korea) and an elemental analyzer (Eurovector, Redavalle, Italy). Scanning electron microscopy (SEM, Hitachi S-4800 with ISIS 310, Japan) was used to investigate the morphology and size of biochar particles. The structural features and surface functionality of the biochar were further determined by: 1) X-ray photoelectron spectroscopy (XPS) analysis (K-Alpha, ThermoFisher, USA), 2) Fourier transform infrared spectroscopy (FTIR) (Frontier, PerkinElmer, USA), and 3) Raman spectrometer (ARAMIS, Horiba Jobin, Japan). Chemical properties of the biochar are presented in the supporting information (Appendix A in Table S2). Further information about the characteristics of the biochar used here is provided in Kim et al. (2016) and El-Naggar et al. (2018).

The soil was treated with rice hull biochar at the rate of 5% (w/w). Both the un-treated soil and biochar-treated soil were incubated in the laboratory at 70% of the water-holding capacity for six weeks. At the end of the incubation period, the un-treated soil and biochar-treated soil were air-dried, crushed, and passed through a 2-mm sieve, characterized, and used for the subsequent redox experiments. The un-treated soil and biochar-treated soil, as well as certified reference soils, were digested by HCl and $HNO_3$ using a microwave (Milestone; ETHOS EASY, Germany) for the determination of the pseudo-total element concentrations (USEPA, 2007).

### 2.2. Automated biogeochemical microcosm experiment

An automated biogeochemical microcosm system (MC) was employed to simulate the flooding of the un-treated soil and biochar-treated soil in the laboratory by controlling the redox conditions. This specialized equipment enabled us to adjust the $E_H$ to pre-defined conditions, which allows for the simulation of various oxic/anoxic cycles that may occur in natural wetlands. Technical details of this set-up are reported in Yu and Rinklebe. (2011). This system has been successfully utilized in previous studies on the release dynamics of PTEs in soils (e.g., Rinklebe et al., 2016a,b; Shaheen et al., 2014, 2016, Shaheen et al., 2020; Frohne et al., 2011; El-Naggar et al., 2019). Briefly, eight MC vessels were used for the un-treated soil and biochar-treated soil (four independent replicates each). Each glass vessel was filled with 210 g of air-dried soil and 1680 mL of tap water to reach a soil/water ratio of 1:8, and hermetically sealed with an air-tight lid. The slurry in each MC was continuously stirred to achieve homogeneity. The system is equipped with an automatic-valve gas regulation system which allows automatic control of $E_H$ by adding nitrogen to lower $E_H$ or oxygen/synthetic air to increase $E_H$. The values of $E_H$ and pH for the MCs were recorded every 10 min via a data logger. We fluctuated the $E_H$ values in two redox cycles to study the impact of the directions of systematic changes of $E_H$ on the release dynamics of the four elements. At first, after flooding, the redox potential was forced from reducing to oxidizing conditions and thereafter from oxidizing to reducing conditions by flushing with oxygen and nitrogen, respectively (Table S3). The dissolved and colloidal fractions of Ag, Sb, Sn, and Tl, in addition to the controlling factors (DOC, DAC, Fe, Mn, $Cl^-$, and $SO_4^{2-}$), were gained separately.

There is still an ongoing debate of the terms “dissolved” and “colloidal”. A number of different definitions for the colloidal and dissolved fractions currently exist (Guo et al., 2007; Löv et al., 2018). For example, Weber et al. (2009) reported that colloids are operationally defined as particles passing the open-pore suction cup (nominal pore size 10–16 μm). Guo et al. (2007) reported that “dissolved fraction” is defined as submicron particles which have a diameter < 0.45 μm and can passes through 0.45 μm filter membrane, while the “Truly Dissolved fraction” is defined as submicron particles which have a diameter < 0.001 μm (1 nm), and includes the hydrated ions and low molecular weight fraction. However, Abgottspon et al. (2015) obtained the dissolved fraction by filtration the solution using 0.02 μm and obtained colloidal + dissolved fraction by filtration the solution using < 10 μm filter membrane; then they considered the difference between both as the colloidal fraction (0.02–10 μm). In our study, we followed the operationally defined dissolved fraction as per (Guo et al., 2007) and filtered the soil suspension after centrifugation through 0.45 μm filter to gather the dissolved fraction while we obtained the colloidal + dissolved by and filtered the filtration soil suspension after centrifugation through 8.0 μm filter (Abgottspon et al., 2015). Then, we considered the difference between concentrations in the 8.0 μm-filtered aliquot, and 0.45 μm-filtered aliquot are assumed to be the colloidal fraction (0.45–8.0 μm). In conclusion, we used the operationally defined fractions as follow: the > 0.45 μm filtrate as dissolved; the < 8.0 μm filtrate as colloidal + dissolved; and the 8.0–0.45 μm filtrate as colloidal. Filtration was carried out using a Millipore membrane (Whatman Inc., Maidstone, UK). All process has been done in a glove box (MK3 Anaerobic Work Station, Don Whitley Scientific, Shipley, UK). The total incubation period was approximately 16 days (375 h). Details of the used methodology and subsampling are provided in the supporting information (Appendix A). The defined $E_H$ windows are listed in Table S3.

### 2.3. Potential mobility of Ag, Sb, Sn, and Tl

The synthetic precipitation leaching procedure (SPLP) is designed to determine the mobility of both organic and inorganic analytes present in liquids, solids, and wastes (Hageman et al., 2000). The synthetic SPLP was used according to the Environmental Protection Agency (EPA) Method SW846/1312 (Hageman et al., 2000) to assess the mobility of Ag, Sb, Sn, and Tl in the bulk soil (non-treated soil and biochar-treated soil) and soil sediment collected under different reducing/oxidizing conditions. An extraction solution consisting of nitric acid and sulfuric acid (60/40 wt%) at pH 4.2 ± 0.05 was added to the soil sediment samples at a liquid-to-solid ratio of 20 L $kg^{-1}$ and shaken in an end-over-end rotator for 18 h.

After extracting the elements mobility, the samples were centrifuged at 4000 rpm for 10 min and filtered with a 0.45-μm membrane filter using disposable syringes. The same procedure was used by Beiyuan et al. (2017), El-Naggar et al. (2018; 2019) to extract the mobility of different trace elements including As, Cd, Cr, Cu, Mo, Pb, Se, and Zn.

### 2.4. Chemical analyses, quality control and data analysis

Concentrations of Ag, Sb, Sn, Tl, Fe, Mn and S in the dissolved and colloidal fractions were analyzed using ICP-OES (Ultima 2, Horiba Jobin Yvon, Unterhaching, Germany). The DOC, total carbon (TC), and total nitrogen (TN) were measured using a C/N-analyzer (Analytik Jena, Jena, Germany). The Specific UV absorbance (SUVA) of the soil solutions was measured at 254 nm using a UV/VIS spectrophotometer (CADAS 200, Dr. Lange, Germany). The SUVA was calculated by normalizing the determined 254-nm absorbance to the concentration of DOC according to Weishaar et al. (2003) Concentrations of $Cl^-$ and $SO_4^{2-}$ in the dissolved fraction were measured using an ion chromatograph (Personal IC 790, Metrohm, Filderstadt, Germany) with a Metrosep A Supp 4 - column (Metrohm, Filderstadt, Germany). The detection limit was 0.03 mg L-1.

Blank and triplicate or quadruplicate measurements were employed

in all analyses to ensure the validity of data. Certified reference materials of the soil and standard solutions (Merck) were used to guarantee high-quality results. Quality control of the extraction efficiency of the pseudo-total element concentrations was performed using certified soil reference materials (CRM051 and CRM042) obtained from Labmix24 GmbH, Germany. The maximum relative standard deviation (RSD) between replicates was set to 5%. Values above 5% were not included in the statistical analyses.

Statistical analyses were carried out using IBM SPSS Statistics version 25 (NY, USA). Factor analysis was carried out as Principal Component Analysis, and the number of interaction calculations was limited to 25. OriginPro 9.1 b215 (OriginLab Corporation, Northampton, USA) was used to calculate the regression equations and the coefficients of determination ($R^2$), and to create the figures. Further details concerning the quality assurance of the collected results and statistical analyses are provided in the supporting information (Appendix A).

## 3. Results and discussions

### 3.1. Properties and pseudo-total element content of the studied soil and biochar

The studied soil contains 77.7% sand and 1.5% clay. The soil is slightly alkaline and contains salts (pH = 7.4; EC = 7.2 $dSm^{-1}$). The soil is poor in total carbonates (1.0%) and total organic carbon (0.38%). $SiO_2$ phase was dominant (58.7%) (Appendix A in Table S1). Results of XPS, FTIR, and Raman analysis of the biochar are presented in Fig. 1 and basic properties and SEM-EDX analysis are given in the supporting information (Appendix A in Table S2 and Fig. S1). The biochar surface contains functional groups including C = O, carbonyl C; C-OH/C-O, hydroxyl C; C-C/C-H, aliphatic/aromatic C; and $sp^2$ C with highly aliphatic and aromatic C components (Fig. 1a,c). Signals between 400 and 800 $cm^{-1}$ were detected (Fig. 1b), which can be related to silicates and/or halogens, as proposed by Trakal et al. (2014) and Liu et al. (2016). The high abundance of H- and O-containing functional groups is evidence for the reactive surface of the biochar. Furthermore, aromatic carbon (C = C) could act as a major electron acceptor in the process of biochar oxidation, which may lead to lower concentrations of basic sites on the biochar surface, (Melo et al., 2019) resulting in new functional groups with Brønsted acid characteristics (El-Naggar et al., 2018). High concentrations of O-containing functional groups on the biochar's surface, such as hydroxyl C (C-O) and carbonyl C (C = O), may lead to an ultimately influencing soil properties upon amendment and the redox-induced mobilization of the studied elements (El-Naggar et al., 2018; Yang et al 2019).

The pseudo-total content of the studied elements in the un-treated soil and biochar-treated soil were 0.68 and 0.62 mg $kg^{-1}$ for Ag, 8.7 and 7.7 mg $kg^{-1}$ for Sb, 12.6 and 12.7 mg $kg^{-1}$ for Sn, and 8.8 and 6.4 mg $kg^{-1}$ for Tl, respectively (Appendix A; Table S1). Those contents were higher than the world soil average and the international maximum allowable concentrations (Kabata-Pendias, 2011). The high pseudo-total contents might be due to mining activities in the area (El-Naggar et al., 2018; Li et al 2019).

### 3.2. Redox potential and pH in soil slurry

The redox potential of the slurry ranged from −30 mV to + 218 mV in the un-treated soil and from −12 mV to + 333 mV in the biochar-treated soil over the entire experimental period (n = 11, 000) (Fig. 2). The pH in the slurry ranged between 6.1 and 8.4 in the un-treated soil and 5.5 and 7.6 in the biochar-treated soil, and decreased under oxic conditions (Fig. 2). An inverse trend between $E_H$ and pH has been previously observed in other soils (e.g., (Rinklebe et al., 2016a,b), involving an increase in $E_H$ which leads to a decrease in pH and vice versa. Alteration of $E_H$ towards reducing conditions, particular in the second redox cycle was accompanied with pH increase, which may possibly due to the consumption of protons required for the reduction of $NO_3^-$, Mn, and Fe (Rinklebe et al., 2016a,b; Frohne et al., 2011).

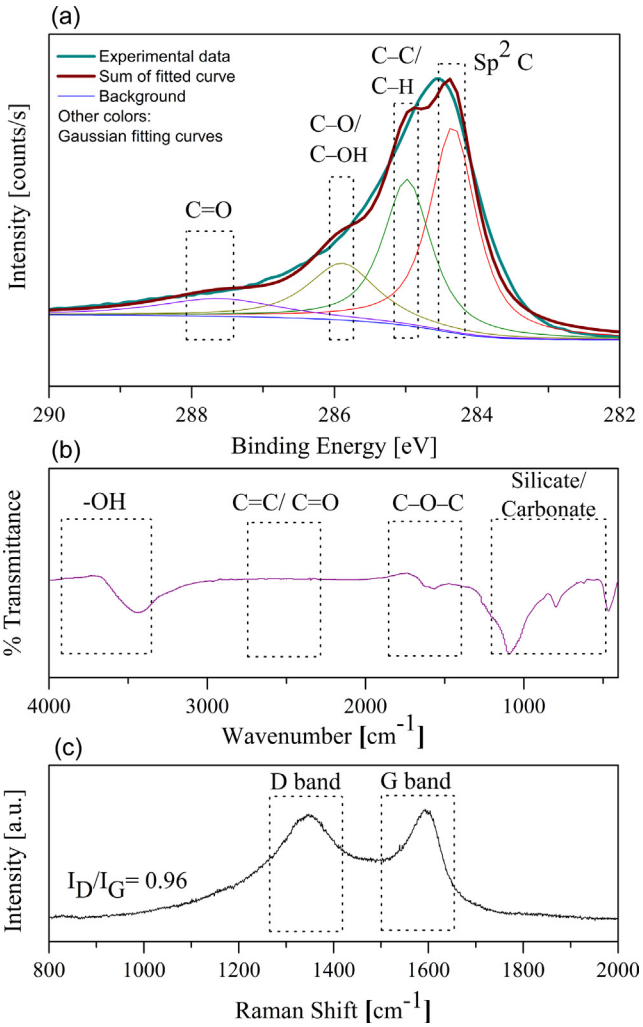


**Fig. 1.** Biochar characterization using a) X–ray photoelectron (XPS) spectroscopy, b) Fourier transform infrared (FTIR) spectroscopy, and c) Raman spectroscopy.

The biochar-treated soil exhibited a wider range of $E_H$ and a lower pH than the un-treated soil, which can be explained by the biochar composition (Fig. 1a,b,c) and redox activity of biochar. Biochar may increase a soil's capacity to accept and/or donate electrons by controlling electron transfer reactions, (Yuan et al., 2017; El-Naggar et al., 2018) thus leading to a wider range of $E_H$ in the soil slurry. Awad et al. (2018) reported about this phenomenon, wherein they postulated that biochar accepted and donated electrons from electron transfer mediators and modulated soil redox processes according to the specific characteristics and pyrolysis temperature of the applied biochar. The formation of carboxylic and oxygenated functional groups at the surface of the biochar may contribute to an increase of the retention of cations and elements in the soil slurry (Awad et al., 2018).

The decrease in pH of the biochar-treated soil (down to 5.5) may result from the oxidation of the biochar's surface at high $E_H$ (+200 to + 300 mV), (Yuan et al., 2017) which would decrease the number of basic sites to the soil slurry and leads to a lower pH (El-Naggar et al., 2018). Also, small organic molecules (after addition of biochar to soil) might be decomposed by soil microorganisms which produce amounts of $CO_2$, organic acids and the release of initial ammonia content, what decrease soil pH. Electro-active biochar components may also

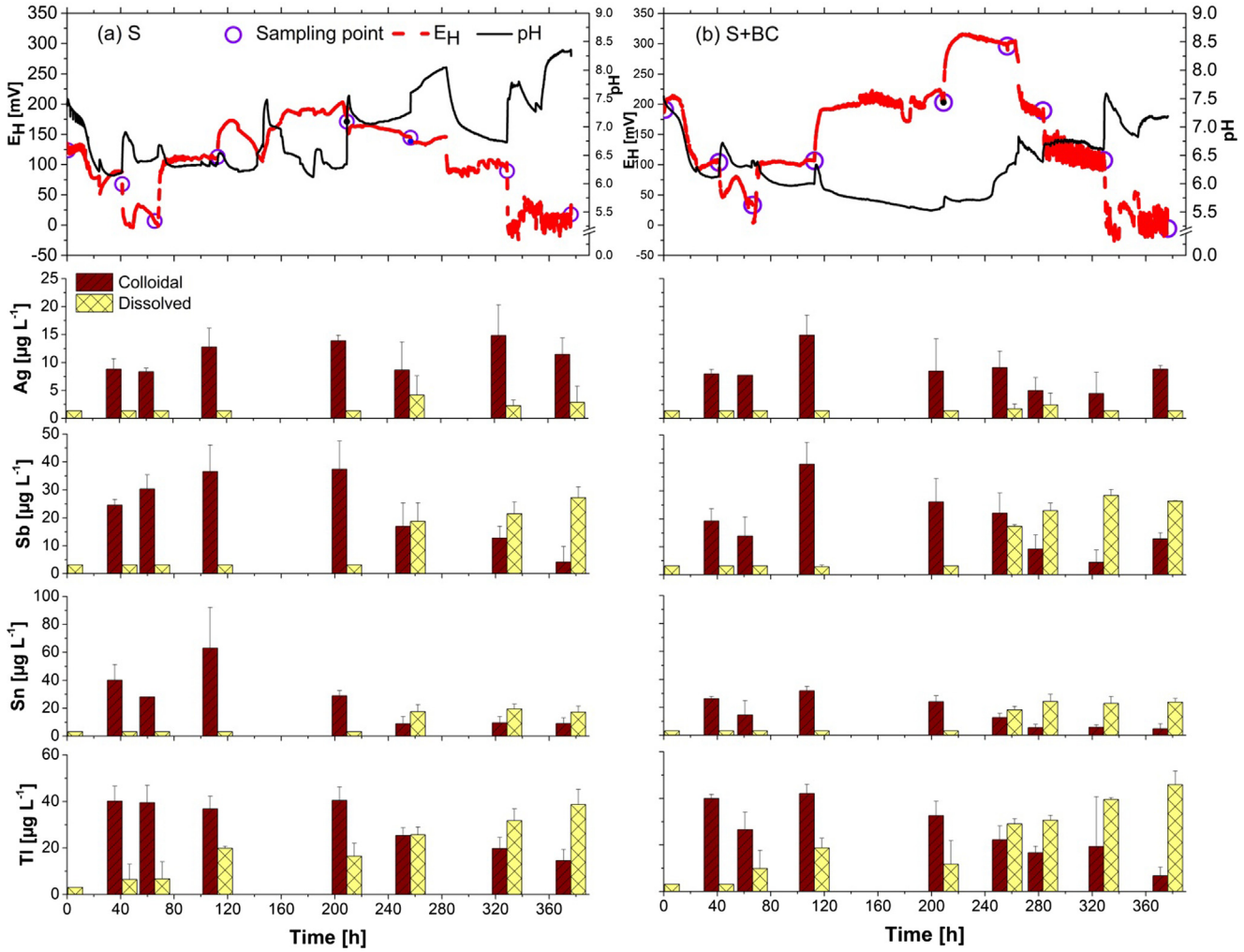


**Fig. 2.** Development of redox potential ($E_H$: solid and red line), pH (dashed and black line), and sampling points (crosses) in the soil slurry, and the mean values of dissolved and colloidal concentrations of Ag, Sb, Sn, and Tl in the non-treated and biochar-treated soil. Data of $E_H$ and pH recorded every 10 min, averages were reported for an underling dataset [n≈11,000] of four replicate samples) in the microcosms of non-treated soil (S; $R^2 = 0.11$; $P < 0.001$), and biochar-treated soil (S + BC; $R^2 = 0.36$; $P < 0.001$). Mean values were calculated from the values of four independent microcosms as four replicates.

contribute to the redox properties of humic substances in soils, which may affect soil pH. Our investigations as well as other works (e.g., Yuan et al., 2017; Klüpfel et al., 2014; Joseph et al., 2010; Joseph et al., 2013) highlight the importance of redox process affecting soil properties occurring on the surface and in the vicinity of biochar particles. Mineral matter, labile organic molecules and C functional groups at biochar surfaces may determine the $E_H$ of a biochar-treated soil (Joseph et al., 2013). Biochar impacts on soil $E_H$ can change over time especially if biochar reacts/interacts with micro-organisms, soil mineral and organic matter (Joseph et al., 2013). It is also possible that as biochar fragment, new redox active surfaces are exposed, thus resulting in a more complex series of redox reactions. Our results imply that the observed wider range of $E_H$ and pH in the biochar-treated soil in comparison to the untreated-soil affect the release dynamics of Ag, Sb, Sn, and Tl (section 3.3).

### 3.3. Dissolved and colloidal concentrations of Ag, Sb, Sn, and Tl

#### 3.3.1. Release of Ag, Sb, Sn, and Tl in the dissolved and colloidal fraction

Thallium was more mobile in comparison to Sb, Sn, and Ag, observed to have the highest dissolved and colloidal concentrations among the four elements, while Ag showed the lowest (Fig. 2; Table 1). Thallium is known to be weakly bound to soil components (Jacobson et al., 2005; Vaněk et al., 2016). Increasing Tl mobilization in the studied soil may increase its concentrations in the ground water and also increase its uptake by plants, which consider as a major environmental issue and threat to human and the ecosystem health, because the human exposure to Tl is mainly associated with the consumption of contaminated food or drinking water.

On the contrary, Sb is relatively more immobile than Tl in the natural environment due to its precipitation with alkali metal(loid)s which results in the formation of stable mineral phases, such as calcium antimonates (Herath et al., 2017). The fairly low observed solubility of Sn indicates that inorganic Sn is relatively immobile and tends to accumulate in soils (Kabata-Pendias, 2011).

Silver was more abundant in the colloidal fraction than in the dissolved fraction at all studied $E_H$ values during the entire experimental period in both the biochar-treated and un-treated soil (Fig. 2), which indicate that Ag might be associated with soil colloids under different redox cycles. We assume that Ag may have high affinity to soil colloids (such as clay, Fe oxides, and organic materials). Silver has been shown to be relatively immobile in soils and tends to be retained by soil compounds such as clay, Fe oxides, and organic materials under a wide range of soil pH (Jacobson et al., 2005; Sikora and Stevenson, 1988). Exchange reactions are purported to play an important role in $Ag^+$ sorption to soils. Among soil colloids, organic colloids content could be a dominant factor in Ag sorption in soils. This behavior is consistent with the reportedly strong complexation of Ag by humic and fulvic

**Table 1**
Variations of concentrations of elements and carriers in the dissolved and colloidal fractions as well as pH and redox potential ($E_H$) in suspensions of the non-treated soil and the biochar-treated soil (number of analyzed sample s are 28 in soil and 32 in soil + biochar).

| Parameter | Unit | Minimum | Maximum | Mean | SD | Minimum | Maximum | Mean | SD |
|---|---|---|---|---|---|---|---|---|---|
| | | Dissolved | | | | Colloidal | | | |
| | | Soil | | | | | | | |
| Ag | [µg $L^{-1}$] | 1.4 | 8.3 | 2.1 | 1.8 | 4.3 | 22.7 | 11.2 | 3.9 |
| Sb | | 3.1 | 30.7 | 11.4 | 10.4 | 0.65 | 51.6 | 23.2 | 13.3 |
| Sn | | 3.1 | 24.4 | 9.5 | 7.9 | 2.4 | 98.8 | 26.7 | 21.8 |
| Tl | | 3.1 | 45.0 | 20.8 | 12.4 | 8.2 | 48.5 | 30.9 | 11.3 |
| DOC | [mg $L^{-1}$] | 261.5 | 2593.0 | 1596.8 | 930.5 | 10.6 | 406.6 | 155.5 | 138.4 |
| SUVA | [L $cm^{-1}$ $mg^{-1}$] | 0.001 | 0.018 | 0.006 | 0.006 | 0.000 | 0.054 | 0.0043 | 0.014 |
| Fe | [mg $L^{-1}$] | 0.05 | 0.25 | 0.12 | 0.06 | 0.03 | 0.66 | 0.19 | 0.14 |
| Mn | | 0.07 | 1.7 | 0.94 | 0.47 | 0.00 | 2.1 | 0.21 | 0.55 |
| $SO_4^{2-}$ | | 440.5 | 896.2 | 702.1 | 141.4 | nd | nd | nd | nd |
| $Cl^-$ | | 870.1 | 1296.7 | 1055.2 | 123.7 | nd | nd | nd | nd |
| | | Soil + Biochar | | | | | | | |
| Ag | [µg $L^{-1}$] | 0.79 | 5.5 | 1.5 | 0.79 | 0.37 | 19.6 | 8.2 | 4.1 |
| Sb | | 1.95 | 29.9 | 12.4 | 10.6 | 1.3 | 50.9 | 19.3 | 11.5 |
| Sn | | 3.13 | 29.8 | 12.6 | 10.1 | 1.8 | 36.1 | 15.9 | 10.8 |
| Tl | | 3.13 | 50.8 | 23.0 | 15.07 | 2.1 | 51.1 | 25.6 | 13.8 |
| DOC | [mg $L^{-1}$] | 281.67 | 2346.3 | 1661.1 | 607.1 | 0.47 | 168.5 | 59.1 | 46.9 |
| SUVA | [L $cm^{-1}$ $mg^{-1}$] | 0.0015 | 0.014 | 0.003 | 0.003 | 0.000 | 0.0028 | 0.0003 | 0.0006 |
| Fe | [mg $L^{-1}$] | 0.03 | 0.37 | 0.11 | 0.07 | 0.03 | 2.6 | 0.30 | 0.48 |
| Mn | | 0.81 | 3.71 | 2.19 | 0.80 | 0.01 | 2.7 | 0.29 | 0.69 |
| $SO_4^{2-}$ | | 362.55 | 782.3 | 605.5 | 96.7 | nd | nd | nd | nd |
| $Cl^-$ | | 756.47 | 1338.8 | 1058.5 | 123.3 | nd | nd | nd | nd |

$E_H$ = Redox potential; DOC = dissolved organic carbon; SUVA = Specific UV absorbance: calculated as the absorbance (measured at 254 nm) normalized to the DOC; SD: standard variation; Min: Minimum; Max.: Maximum; nd: not determined

acids, and by soil organic matter, especially thiol groups (Jacobson et al., 2005).

On the other hand, Sb, Sn, and Tl revealed a similar behavior and were more abundant in the colloidal fraction than in the dissolved fraction in the first redox cycle (decreasing $E_H$ from the initial (+200 mV) to −30 mV; then increasing $E_H$ from −30 mV to + 333 mV). However, in the second redox cycle (decreasing $E_H$ from + 333 mV to 0 mV), the three elements were more abundant in the dissolved fraction than in the colloidal fraction in both the un-treated soil and the biochar-treated soil (Fig. 2). This result indicates that Sb, Sn, and Tl are retained by colloids under oxic acidic conditions in the first redox cycle (in particular in the biochar-treated soil) and released to soil solution in the second redox cycle under moderately reducing and alkaline conditions (Fig. 2). These results indicate that colloids might play an important role in Ag, Sb, Sn, and Tl mobilization in the studied soil, as will be discussed in section 3.3.2.4.

Biochar application to the soil leads to a relative increase of the release of dissolved Sb, Sn, and Tl, and to a relative decrease of the colloidal concentrations in comparison to the un-treated soil (Table 1; Fig. 2). The wider range of $E_H$ (-12 to + 333) and pH (5.0–8.1) in the biochar treated soil than the un-treated soil ($E_H$ = -30 to + 218; pH = 5.9–8.6) might be a potential factor in increasing the solubility of the elements in the biochar treated soil in comparison to the un-treated soil. Redox properties of the biochar and the related processes may impact the mobilization of Sb, Sn, and Tl in the biochar-treated soil. In particular, functional groups in biochar contribute to its redox characteristics, where these groups may act as both electron donor and acceptor, reducing and oxidizing the elements, which affect the elements reduction and oxidation in the flooded soil (Yuan et al., 2017; Dong et al., 2014). For example, semiquinone radicals in the biochar might be involved in the metal(loi)d oxidation, while the carboxylic groups in the biochar may participate in both reduction and oxidation of the elements (Yuan et al., 2017; Xu et al., 2019; Shaheen et al., 2019; Wang et al., 2010). The spectroscopic characterization of the studied biochar (Fig. 1) indicated high abundance of H, C, and O-containing functional groups. While the functional groups such as phenolic species in biochar are the main electron donating moieties (i.e., reducers), the quinones and polycondensed aromatic functional groups are the components accepting electrons (oxidants). Therefore, we assume that the used biochar might be rich in π-electrons due to the abundance of surface functional groups and these groups may act as electron donors for the Sb, Sn, and Tl reduction reactions, and thus biochar may play an important role in reducing $Tl^{3+}$ to $Tl^+$, $Sb^{5+}$ to $Sb^{3+}$, and $Sn^{4+}$ to $Sn^{2+}$, which increase their solubility under reducing conditions as compared to oxic conditions (Fig. 2).

On other the hand, biochar application to the soil decreased the concentrations of Ag in the dissolved and colloidal fraction especially at the end of the experiment under low $E_H$ and high pH (Fig. 2). The dissolved concentrations of Ag decreased from 1.38 to 8.36 µg $L^{-1}$ in the un-treated soil to 0.79–5.58 µg $L^{-1}$ in the biochar treated soil (Table 1). This could be due to the increase of soil organic carbon in the biochar treated soil and the related sorption of Ag to the organic matter. Biochar has the ability to adsorb Ag by a combination two consecutive mechanisms, reduction and physical adsorption as reported by Antunes et al. (2017). In this respect, Abbas et al. (2019) found that biochar immobilized Ag in paddy soil and thus can be used effectively to prevent its uptake in rice.

These results indicate that the studied biochar might be used for immobilization of Ag and decreasing its plant uptake in the studied soil. However, for the used biochar leads to an increasing mobilization of Sb, Sn, and Tl, which would increase their uptake and movement to the ground water and therefore increase their potential risk in the studied ecosystem. On other side, increasing the dissolved concentration of Sb, Sn, and Tl by biochar might be used for enhancing their phytoextraction using nonedible plants and shorten the requested time for phyto-management of the studied soil.

### *3.3.2. Biogeochemical governing factors*

The differing redox-behaviors of Ag, Sb, Sn, and Tl in the un-treated and biochar-treated soil can be explained by the changes of $E_H$ as well as the linked $E_H$-dependent changes of pH, Fe, Mn (hydr)oxides, S, $Cl^-$, DOC, and DAC. We conducted factor analysis to determine the associations between the concentrations of Ag, Sb, Sn, and Tl and controlling factors ($E_H$, pH, DOC, SUVA, Fe, Mn, S, and $Cl^-$) in the dissolved

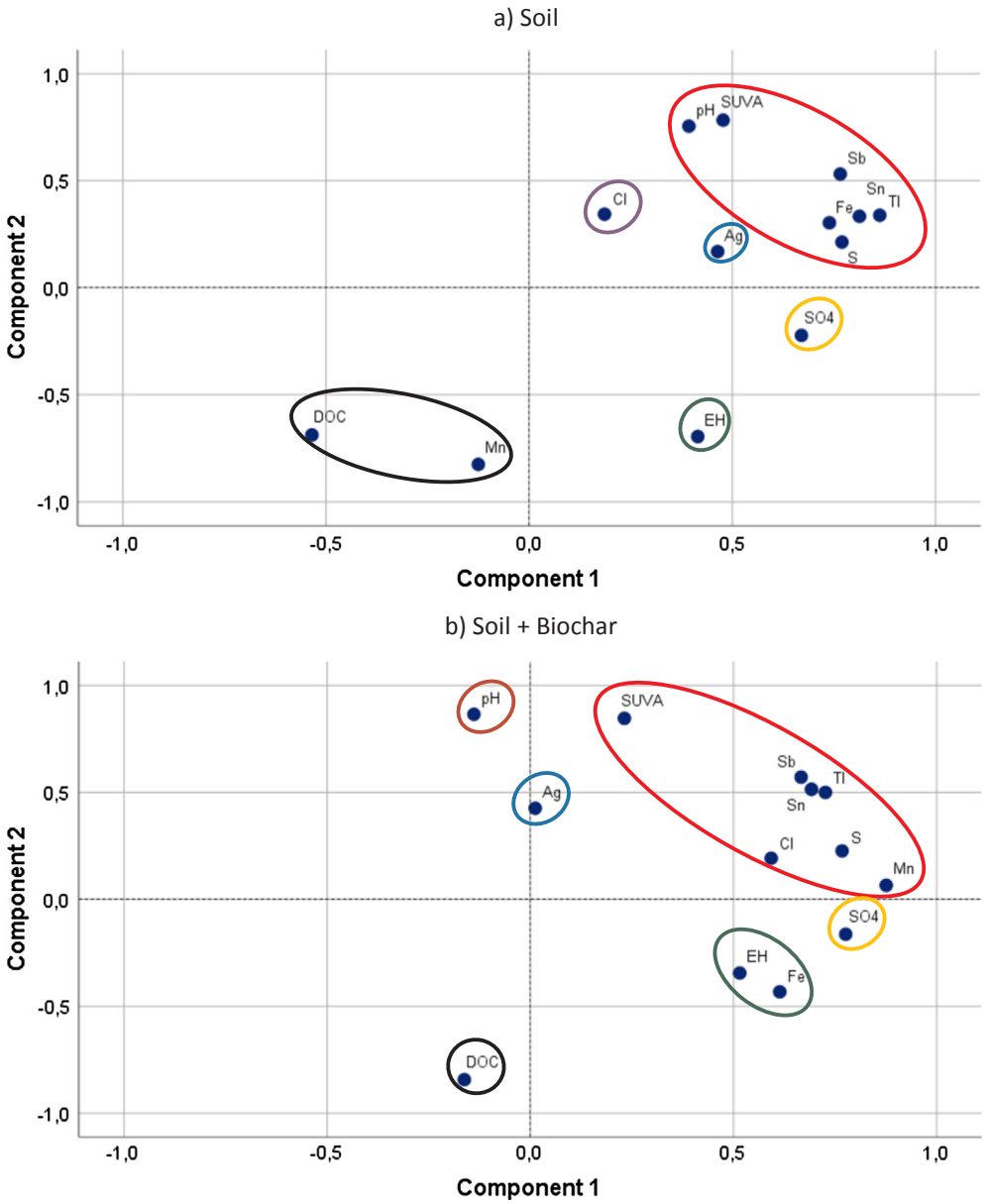


**Fig. 3.** Factor analysis to determine the relationships between the measured dissolved elements and parameters and to identify complex cause-and-effect inter-relationships in the non-treated soil and biochar-treated soil.

fraction, and to identify the complex cause-and-effect interrelationships (Fig. 3a,b). The factor analysis revealed that the dissolved Sb, Sn, and Tl were associated in one cluster, while Ag was separated from the three elements in both the un-treated soil and the biochar-treated soil.

The dissolved concentrations of Ag, Sb, Sn, and Tl clustered separately from $E_H$ but together with S in both soils. The dissolved fractions of Sb, Sn, and Tl grouped together with pH only in the un-treated soil (Fig. 3a). The SUVA clustered with dissolved Sb, Sn, and Tl in one group, while the DOC was separated from this group in both soils. Concentrations of Sb, Sn, and Tl in the dissolved fraction grouped together with Fe in the un-treated soil, and with Mn and $Cl^-$ in the biochar-treated soil (Fig. 3a,b). The total explained variance in the un-treated soil is 64.15% (49.46% Component No. 1 and 14.69% Component No. 2) and in the biochar-treated soil is 62.44% (40.27% Component No. 1 and 22.18% Component No. 2). The most important factors for the formation of component No. 1 in the un-treated soil are Sb, Tl, SUVA, DOC, Sn and followed by pH, Fe, S, Mn and Ag, while the most important factors for the formation of component No. 2 are $E_H$ followed by $SO_4^{2-}$ and Mn. On the other hand, in the biochar-treated soil, the most important factors for the formation of component No. 1 are Tl, Sb, Sn and followed by Mn and S, while the most important factors for the formation of component No. 2 are pH, Fe, followed by DOC, SUVA, and $SO_4^{2-}$. More details about the impact of $E_H$, pH, DOC, SUVA, Fe, Mn, S, and $Cl^-$ on the redox-behavior of Ag, Sb, Sn, and Tl are presented in the following sections.

*3.3.2.1. $E_H$/pH.* The dissolved fractions of Ag, Sb, Sn, and Tl reveal no clear pattern in response to fluctuations of $E_H$; therefore, they were separated from $E_H$ in the factor analysis (Fig. 3a,b). Also, they showed non-significant relations with $E_H$ in both the untreated-soil and in the biochar-treated soil (Appendix A in Table S4). The solubility of Sb, Sn, and Tl decreased at higher $E_H$ (+218 to + 330) and lower pH (5.1–5.9) in the first redox cycle, as compared to in the second redox cycle at lower $E_H$ (-30 to −12 mV) and higher pH (8.1–8.6) (Fig. 2). Soil pH had a positive significant relation to the dissolved fraction of the Sb, Sn, and Tl in the un-treated soil (Table S4), and thus they clustered together (Fig. 3a). These results mean that liming materials may cause an increase in the solubility and mobility of Sb, Sn, and Tl in flooded soils.

The impact of pH on Ag solubility was non-significant in both soils and thus they were separated from each other in the factor analysis (Fig. 3a,b).

We assume that increasing Tl solubility under reducing alkaline conditions might be due to the existence of Tl in the form of the soluble thallous cation $Tl^+$. The $Tl^+$ ion is the dominant species in many $E_H$–pH combinations (Takeno, 2005). In this respect, Casiot et al. (2011) indicated that $Tl^+$ is relatively soluble, and it tends to dominate over $Tl^{3+}$ in aquatic environments, due to the high redox potential of $Tl^{3+}$/ $Tl^+$ couple ($E_H$ = 1.28 V). The dominance of $Tl^+$ in soil solution is reported by Xiong (2007) and Jia et al. (2018) who found that Tl in the solution of rhizosphere mainly exists as $Tl^+$. Jia et al. (2018) also reported that $Tl^{3+}$ can be reduced to $Tl^+$ in soils even at the surface where the chemical environment promotes oxidation. $Tl^{3+}$ is less stable and can undergo rapid electrochemical reduction to $Tl^+$ (logK ≅ 40, $E_{red}(Tl^{3+}/Tl^+) = +1.26$ V (Biaduń et al., 2016).

Also, we assume that the interactions between Tl and potassium (K) in our soil ($K_2O$ = 1.8%; Table S1) may also affect the release and mobilization of Tl. For example, in the reduced state, $Tl^+$ has the same charge as and is comparable in size to $K^+$, with ionic radii of 1.76 Å for $Tl^+$ and 1.60 Å for $K^+$. This allows $Tl^+$ to substitute for similar-sized alkali element $K^+$ in soil minerals (Jacobson et al., 2005; Rader et al., 2019). The high solubility of Tl in our soil may pose human health and ecosystem risks because Tl is a highly toxic element to humans and mammals and also inhibits the growth of many plants and aquatic organisms (Rader et al., 2019).

The relatively higher concentration of dissolved Sb under moderately reducing ($E_H$ = +100 to –33 mV) and alkaline (pH = 8.1–8.6) conditions might be due to the presence of $Sb^{3+}$ and/or $Sb^{5+}$. Findings by Hockmann et al. (2014) indicate that $Sb^{3+}$ is predominant at low redox conditions (Eh < 50 mV) in the solid and liquid phase, while $Sb^{5+}$ is less stable in reducing environments. The presence of $Sb^{5+}$ under a wide range of $E_H$ is reported by Chen et al. (2003), Mitsunobu et al. (2006) and Wan et al. (2013) who indicated that $Sb^{5+}$ can be a stable oxidation state even under reducing conditions. In addition, the mobility of $Sb^{5+}$ is relatively higher compared than $Sb^{3+}$ at neutral pH (Herath et al., 2017; Mitsunobu et al., 2009).

Similar to Tl and Sb, Sn in the colloidal and dissolved fraction was found to be mobilized under wide ranges of $E_H$ and pH (Fig. 2). However, in the second redox cycle, Sn was abundant in the dissolved fraction under low $E_H$. Tin in soil solution might be found in two oxidative states, stannous (Sn (+2)) and stannic (Sn (+4)). Generally, the mobility of Sn is highly $E_H$/pH dependent; especially, Sn (+2), a strong reducing agent, can be present mainly in acid and reducing environments (Kabata-Pendias, 2011). In addition, an enhanced solubility of Sb and Sn under low $E_H$ might be also due to an increased degree of methylation under low $E_H$ as indicated by Frohne et al. (2011) for Sb and by Falke and Weber (1994) for Sn.

The relative increase of Tl, Sb, and Sn solubility in the biochar-treated soil might be caused by functional groups such as phenolic species in biochar which may act as electron donor, and play an important role in reducing $Tl^{3+}$ to $Tl^+$, $Sb^{5+}$ to $Sb^{3+}$, and $Sn^{4+}$ to $Sn^{2+}$, which increase their solubility under reducing conditions. These above-mentioned results failed to identify simple and clear distinct patterns of the four elements in response to fluctuations of $E_H$. This may imply that the redox-induced release of the four elements might be controlled indirectly via the $E_H$-dependent changes in pH and the chemistry of Fe, Mn, S, and DOC as discussed in the following sections.

*3.3.2.2. DOC/SUVa.* The concentrations of organic carbon (OC) were higher in the dissolved than in the colloidal fraction (Table 1). The dissolved OC (DOC) increased under low $E_H$ in the first redox cycle (Appendix A in Fig. S2). The higher DOC at reducing than at oxidizing conditions in the first redox cycle might be due to release of organic matter bound to reductively dissolved Fe- and Mn-hydroxides and/or the release of OC from soluble organic metabolites produced by reducing bacteria under reductive conditions (Frohne et al., 2014). During the second reducing cycle (+100 and 0 mV) the addition of biochar leads to higher values of organic carbon in the dissolved fraction as compared to the un-treated soil (Appendix A in Fig. S2). This might be due to the release of dissolved organic materials from biochar during the second redox cycle after a long flooding period.

The higher SUVA under oxic/alkaline conditions indicates that the proportion of aromatic DOC to aliphatic DOC in the studied soil was higher at high $E_H$ and pH than at low $E_H$ and pH. These results show that aromatic carbon compounds were more resistant and increased under oxidizing conditions, while low molecular weight and labile organic carbon was more easily decomposed under reducing conditions. We assume that desorption of OM sorbed onto soil minerals due to pH change during reduction–oxidation cycles explains the behavior of SUVA in our soil. The protonated hydroxyl groups at low $E_H$ and pH in the tested soil can generate a positive charge on the mineral surfaces, which induces sorption of negatively charged (less aromatic) organic molecules and promotes their surface complex formation. Similar trends and interpretations of SUVA results have been reported by Weishaar et al. (2003) and Shaheen et al. (2014).

The SUVA clustered with dissolved Sb, Sn, and Tl in one group, while the DOC was separated from this group in both soils (Fig. 3a,b). An opposite behavior between SUVA and DOC was also observed in the significant positive relations between SUVA and Sb, Sn, and Tl on one hand and the negative relations between these three elements and DOC on the other hand (Appendix A in Table S4). We hypothesize that aromatic organic compounds are more important than aliphatic organic compounds for governing the release of Sb, Sn, and Tl in the soil. Our used biochar surface contains functional groups includes aliphatic/aromatic C; and $sp^2$ C with highly aliphatic and aromatic C components (Fig. 1), which support our hypothesis. We infer that Sb, Sn, and Tl may form complexes with aromatic organic compounds which are more soluble than their complexes with aliphatic organic compounds. The affinity of some trace elements for DOC might be stronger in solutions containing a greater content of humic and aromatic structures. The ability of such elements to complex with DOC could result in increased mobilization of these elements in the soil environment (Settimio et al., 2014). These results mean that addition of organic materials rich in aliphatic compounds might be used for immobilization of Sb, Sn, and Tl in flooded soils, while using organic materials rich in the aromatic compounds can be used for increasing the mobilization of these elements.

*3.3.2.3. Fe/Mn.* The higher concentrations of colloidal Fe than dissolved Fe in both the un-treated soil and in the biochar-treated soil (Table 1) indicate that Fe might be relatively more associated with colloids. In contrast, Mn was more abundant in the dissolved than the colloidal fraction (Table 1), in particular under oxic conditions (Appendix A in Fig. S2), which might be explained by the associated decrease of pH as indicated by Takeno (2005) and explained by Shaheen et al. (2014). The dissolved concentrations of Sb, Sn, and Tl were associated with Fe in the un-treated soil, and with Mn in the biochar-treated soil, while Ag was associated with neither Fe nor Mn in both soils (Fig. 3a,b). The association revealed by factor analysis between dissolved concentrations of Sb, Sn, and Tl and dissolved Fe in the un-treated soil, and with Mn in the biochar-treated soil, can be explained by the reductive dissolution of Fe-Mn(hydro)oxides under low $E_H$ and release of the associated Sb, Sn, and Tl to soil solution in the dissolved form. These findings are consistent with a stronger impact of Fe redox chemistry on elemental solubility in the un-treated soil than in the biochar-treated soil. On the other hand, the impact of Mn redox chemistry on the dissolved elements seems higher in the biochar-treated soil than the untreated soil, which may be due to the higher redox sensitivity of Mn oxides and the wider range of $E_H$ and a lower pH in the biochar-treated than in the un-treated soil. The reductive dissolution of Fe and Mn oxides does not occur simultaneously,

where Mn oxides reduce before Fe; this may explain that Mn is relatively more abundant in the dissolved phase compared to Fe, and this may explain that Sb, Sn, and Tl associate with Fe in the un-treated soil but with Mn in the biochar-treated soil.

The interaction between Sb and Fe is in agreement with those reported by Hockmann et al. (2014), Wan et al. (2013), and Han et al. (2018) who found that previously sorbed $Sb^{3+}$ can be gradually released to the soil solution due to reductive dissolution of iron (hydr) oxides under reducing conditions. The positive relations between Sn and Fe were in agreement with Kabata-Pendias (2011) who reported that the mobility of Sn in soils is rather similar to that of Fe. The interaction of Tl with Fe and Mn would then be due to the sorption of Tl to $Fe^{3+}$-colloids (Griffiths, 1992). In contact with certain $Mn^{4+}$-oxides, $Tl^{+}$ can be oxidized to $Tl^{3+}$-complexes and stabilized by incorporation into $Mn^{4+}$-oxide (Peacock and Moon, 2012; Voegelin et al., 2015). Previous studies (e.g., Peacock and Moon, 2012; Nielsen et al., 2013) have shown that $Tl^{3+}$ would be stabilized in soils by incorporation into $Mn^{4+}$-oxides, or as $Tl_2O_3$ in soils contaminated with $Tl^{+}$-bearing metal sulfides.

*3.3.2.4. Sulfur and chloride.* Concentration of $SO_4^{2-}$ in the dissolved fraction of the biochar-treated soil was lower than in the un-treated soil (Table 1), indicating that the biochar might have prevented the release of $SO_4^{2-}$ into soil solution. Under the first redox cycle, the concentrations of $SO_4^{2-}$ under oxic conditions were higher than under reducing conditions (Appendix A in Fig. S2); This is most likely because sulfides were formed under reducing conditions and oxidized to $SO_4^{2-}$ under oxic conditions (Takeno, 2005). Concentrations of $Cl^{-}$ reveal very small fluctuations during the experiment and were relatively similar between the un-treated soil and the biochar-treated soil (Appendix A in Fig. S2), with mean values of 1055 and 1058 mg $L^{-1}$, respectively (Table 1), which indicates that the biochar application to soil was not able to retain $Cl^{-}$ and thus, a release of dissolved $Cl^{-}$ from the soil solids into soil solution was detected.

Concentrations of Sb, Sn, and Tl in the dissolved fraction were grouped together with sulfur in the un-treated and the biochar-treated soil (Fig. 3a,b). The correlation analysis also showed that the three elements were positively correlated with sulfur in both soils; Tl was also correlated positively with $SO_4^{2-}$ in both soils (Appendix A in Table S4). These results indicate that the redox chemistry of sulfur may greatly affect the redox-induced release dynamics of Sb, Sn, and Tl and in particular Tl in our soils. In the biochar-treated soil, $Cl^{-}$ was clustered with the Sb, Sn, and Tl (Fig. 3b) while $SO_4^{2-}$ forms a separate cluster, which could be interpreted as an indication that the elements might form complexes with $Cl^{-}$ ions in our salt-affected soil. We may conclude that Tl(+1) may be able to form relatively strong complexes with $Cl^{-}$ and weaker complexes with $SO_4^{2-}$, as also reported by Evans and Barabash. (2010). Under reducing conditions, thallium sulfide, $Tl_2S$(s), might be formed, which is relatively soluble compared to other metallic sulfides (Evans and Barabash., 2010). We also found that the sulfide fraction of Tl is dominant in both the soil and biochar-treated soil (data not shown). The importance of sulfides and chloride on the leachability of Tl is reported by others (e.g., Antić-Mladenović et al., 2017; Karbowska et al., 2014).

The association between the dissolved Sn and sulfur in the solution of both soils (Fig. 3a,b) could be due to a variety of Sn sulfide minerals which may exist in our soil, such as stannite ($Cu_2SnFeS_4$) and montesite ($PbSn_4S_5$) as mentioned by Kabata-Pendias (2011) The dominance of the sulfide fraction of Sn in our soil might support the association between Sn and S (data not shown). The impact of sulfide on the release of Sb in our soils can be explained by the ability of dissolved sulfide to reduce $Sb(OH)^{6-}$ under a variety of environmentally relevant concentrations and conditions (Polack et al., 2009). In this respect, Han et al. (2018) also found that the dominant reaction process of Sb under anoxic conditions was its precipitation as sulfide minerals.

We assume that sulfur and chloride are important factors govern the release of Ag in our soil. Silver was separated in the factor analysis from the $E_H$, pH and the other studied factors and did not correlate with these factors (Appendix A in Table S4); however, it was more closely associated to S, $Cl^{-}$, and $SO_4^{2-}$ in the un-treated soil (Fig. 3a). This might be due to the ability of Ag to form strong sulfide complexes (Adams and Kramer, 1998; Hashimoto et al., 2017). In addition, Ag(+1) may sorb onto and into colloidal or particulate sulfides and form $Ag_2S$(s) (Bell and Kramer., 1999). Moreover, Ag ions may be adsorbed rapidly onto amorphous FeS (Evans and Barabash, 2010). Silver also might be precipitated as AgCl(s) under oxidizing conditions and $Ag_2S$(s) under reducing environments. Hashimoto et al. (2017) found that 83% of the spiked Ag in soils was transformed into $Ag_2S$ under reducing conditions. The formation of the precipitate depends on the relative amount of chloride and sulfide in the soil-slurry-system. The XANES results of Settimio et al. (2014) indicated that the added $Ag^{+}$ was reduced to metallic Ag over time, and associations with Fe-oxohydroxides and reduced sulfur groups in organic matter also decreased the lability of Ag. Recently, Van Koetsem et al. (2018) demonstrated that the solid–liquid partitioning of elemental Ag nanoparticles in soils is influenced by soil properties such as pH, CEC, texture, total nitrogen, total phosphorus, suspended matter, total organic carbon and main and trace elements content. The native Ag(s) species dominates a large portion of the $E_H$-pH diagram of Ag; however, under reducing conditions the dominant form of Ag under both acidic and alkaline conditions is the precipitate $Ag_2S$(s) (Takeno, 2005). The $Ag_2S$ is stable and does not dissolve even after prolonged aeration (Auvinen et al., 2017). We assume that under the high salinity and high content of total sulfur (2877 mg $kg^{-1}$) in our soil, Ag(+1) may form precipitates with $Cl^{-}$ under oxic conditions and participates perhaps as $Ag_2S$(s) as suggested by Evans and Barabash. (2010) Thus, these are likely mechanisms for the low degree of Ag solubility and its higher abundance in the colloidal than in the dissolved fraction under our experimental conditions (Fig. 2).

*3.3.2.5. Redox mediated interactions between soil colloids and release of Ag, Sb, Sn, and Tl.* Colloids comprised of silicate minerals, amorphous Fe-oxyhydroxides, organic materials and sulfides/sulfates are important sorbents of pollutants in soils. Collide-metal formation and compositions are strongly affected by redox fluctuation as the change of Fe redox chemistry, pH, ionic strength, and organic matter (Yan et al., 2016). As mentioned above and indicated in Fig. 1, Ag was more abundant in the colloidal fraction than in the dissolved fraction at all $E_H$ windows in both the biochar-treated and un-treated soil. Also, Sb, Sn, and Tl were more abundant in the colloidal fraction than in the dissolved fraction under wide range of $E_H$ and pH, particularly in the first redox cycle (Fig. 1). In addition, Fe concentrations were higher in the colloidal fraction than that of the dissolved fraction in both the un-treated soil and in the biochar-treated soil (Table 1). However, DOC concentrations were higher in the dissolved than in the colloidal fraction (Table 1). Therefore, we assume that the Fe oxyhydroxides and dissolved organic matter (DOM) are the most important colloids can govern the redox-induced release of Ag, Sb, Sn, and Tl in the studied biochar treated and untreated soil. In redox-dynamic soils, colloids mobility is largely controlled by $Fe^{3+}$ dissolution, shifts in pH, and interactions with DOM (Yan et al., 2016). For example, some studies (e.g, Ryan and Gschwend, 1994; Thompson et al., 2006) reported that dispersion of colloids in soils under aerobic/anaerobic conditions has been linked to Fe dissolution and an increase in the suspension pH. Fe oxides can act as cementing agents, binding colloids together or to the soil matrix, and colloids may be released after the dissolution of these oxides. In our soil, Fe dissolution under anaerobic conditions coincided with the initial high level of DOC may lead to subsequent colloid aggregation due to bridging (Yan et al., 2016). However, the high concentrations of DOC released under anaerobic conditions may decrease the colloids release due to DOC–colloid association. This complexity might be explained by the coupling

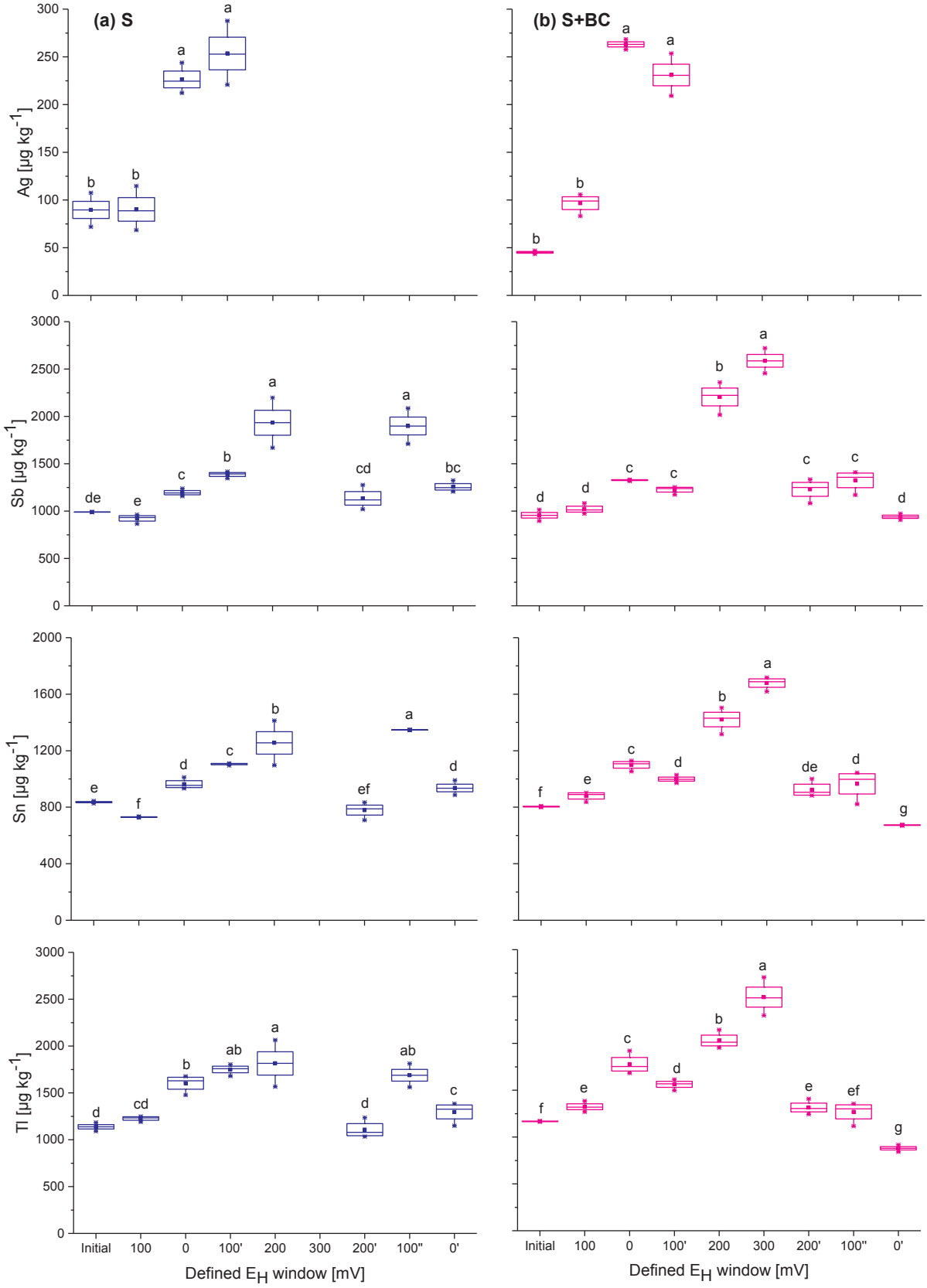


**Fig. 4.** Potential mobility of Ag, Sb, Sn, and Tl in the sediment phase of the non-treated soil (S) and the biochar-treated soil (S + BC) under dynamic $E_H$ conditions. The red dashed line represents the potential mobility of each element in the bulk soils (S and S + BC). Columns represent mean and whiskers represent standard deviation of four replicates using biogeochemical microcosm systems. Values accompanied by different letters are significantly different within columns at the level ($P < 0.05$). Please notice the different scales.

effects of DOM through direct contacts with colloids or indirect influence on microbial Fe reduction via electron shuttling and Fe(II) and Fe(III) complexation (Royer et al., 2002). Baalousha (2009) showed that DOM could both disintegrate soil aggregates into colloids and destabilize (i.e., cause formation of aggregates) suspended colloids depending on the DOM concentration or composition. The dominance of Ag, Sb, Sn, and Tl together with Fe in the colloidal fraction under wide range of $E_H$ and pH in the untreated and biochar-treated soil indicate that the Fe oxides colloidal particles were able to scavenge Ag, Sb, Sn, and Tl (e.g., by sorption) from soil solution, and this might be responsible for decreasing the dissolved concentrations of these elements and increasing their concentration in the colloidal fraction. Increasing the concentrations of Sb, Sn, and Tl in the colloidal fraction under oxic conditions might be explained by the association of these elements with the precipitated Fe oxides and/or with the aromatic compounds of DOC as indicated by the increase of colloidal Fe and SUVA under high $E_H$, which may support our previous hypothesis. These findings have implications for colloid release and colloid-associated mobilization and transport of Ag, Sb, Sn, and Tl in redox-dynamic environments.

### 3.4. Redox-induced potential mobility of Ag, Sb, Sn, and Tl

Thallium and Sb exhibit higher potential mobility than Sn and Ag (Fig. 4). The potential mobility of the four elements, particularly Sb, Sn, and Tl increased with increasing $E_H$ from 0 mV to + 200 mV in the un-treated soil and from 0 mV to + 300 mV in the biochar-treated soil in the first redox cycle. Thereafter, the potential mobility decreases along with decreasing of $E_H$ to 0 mV in the second redox cycle (Fig. 4). The highest potential mobility of Sb, Sn, and Tl in the untreated soil and biochar treated soil was observed at high $E_H$ (+300 mv) and low pH (pH = 5.7), and the lowest at low $E_H$ (0 mv) and high pH (7.2) in the second redox cycle (Fig. 4). These findings mean that the potential mobility of the elements varied under the wider range of $E_H$ and pH in the untreated soil and biochar-treated soil; however, the variations were wider in the biochar-treated soil than the untreated soil. The higher $E_H$ and the associated lower pH increased the potential mobility of the elements in the soil as compared to the moderate reducing alkaline conditions.

Biochar addition leads to a higher potential mobility (Fig. 4) of Sb, Sn, and Tl under oxic redox conditions (+200 and + 300 mV) as compared to the un-treated soil, likely due to the decreased soil pH caused by a higher $E_H$. Those results demonstrate that redox cycles profoundly affect the potential mobility of the studied elements as a result of the $E_H$-dependent changes of soil pH. We assume that the wider range of $E_H$ and pH in the biochar-treated soil than the untreated soil might be a reasonable factor for the higher potential mobility of the elements in the biochar-treated than the untreated soil. Additionally, an enhancement of the total and dissolved organic carbon in the biochar-treated soil in comparison to the untreated soil may contribute to the increase in potential mobility of the elements in the biochar-treated soil at oxic acidic conditions.

## 4. Conclusions

This study demonstrates the high potential of the used automated biogeochemical microcosm system as a powerful tool for understanding the redox-induced mobilization of emerging contaminants in soils, and the utility of such information in environmental and health-related planning and in management of PTEs contaminated wetland soils. We found that the dissolved concentrations and potential mobility of Sb, Sn, and Tl increased in the biochar treated soil, in particular in the second redox cycle. This can increase their release and transfer into the groundwater and the food chain, which could cause negative effects on human and environmental health. The redox activity of biochars in soils could be a function of the changes in pH and Fe chemistry and thus the metals mobilization.

In conclusion, our findings suggest that a release of Sb, Sn, and/or Tl in rice husk biochar treated mining soils should be considered due to an increased mobilization and the associated environmental risks when using those soils for flooded agricultural systems, such as in rice paddy soils and/or fish-culture systems. Also, our results might be useful for a proper management of Ag, Sb, Sn, and/or Tl contaminated wetland soils. For example, our results indicate that the rice hull biochar might be used for the immobilization of Ag and decreasing its plant uptake in the studied soil, while it might be used for enhancing the phytoextraction of Sb, Sn, and Tl. In addition, based on our results, we may suggest using organic materials rich in aliphatic compounds for immobilization of Sb, Sn, and Tl in flooded soils.

Our results provide new insights into biogeochemical processes that control the release dynamics and distribution of Ag, Sb, Sn, and Tl among the dissolved and colloidal fractions of soil solution, as well as the potential mobility of these metal(loi)ds in the solid phase. Further understanding of these processes provides the basic knowledge, so far lacking, to understand, to predict, to control and to remediate Ag, Sb, Sn, and/or Tl polluted flooded soil ecosystems. Speciation of the elements in the soil solution and solid-phase of further soils treated with various types of biochars under dynamic redox conditions is needed in future to gain a deeper understanding of biogeochemical mechanisms controlling the redox-induced release kinetics of these elements and their interactions with biochars.

## Author contributions

**Jörg Rinklebe:** Conceptualization, Data curation, Formal analysis, Funding acquisition, Investigation, Methodology, Project administration, Resources, Software, Supervision, Validation, Visualization, Writing - original draft, Writing - review & editing. **Sabry M. Shaheen:** Conceptualization, Data curation, Formal analysis, Funding acquisition, Investigation, Methodology, Software, Validation, Visualization, Writing - original draft, Writing - review & editing. **Ali El-Naggar:** Data curation, Formal analysis, Investigation, Methodology, Software, Validation, Visualization, Writing - review & editing. **Yong Sik Ok:** Funding acquisition, Project administration, Resources, Supervision, Validation, Visualization, Writing - review & editing. **Hailong Wang:** Validation, Writing - review & editing. **Gijs Du Laing:** Validation, Visualization, Writing - review & editing. **Daniel S. Alessi:** Validation, Visualization, Writing - review & editing.

## Acknowledgments

We thank the German Alexander von Humboldt Foundation (Ref 3.4 - EGY - 1185373 - GF-E) for financial support of the experienced researcher's fellowship of Prof. Dr. Shaheen at the University of Wuppertal, Germany. Also, we thank the National Research Foundation of Korea (NRF-2015R1A2A2A11001432) for the financial support. The authors thank Dr. Tian-ran Li and Prof. Jian-guo Jiang from the School of Environment at Tsinghua University, China for their help in soil sampling, and Mr. C. Vandenhirtz for technical assistance.

## Appendix A. Supplementary data

Supplementary data to this article can be found online at https://doi.org/10.1016/j.envint.2020.105754.

## References

Abbas, Q., Liu, G., Yousaf, B., Ali, M.U., Ullah, H., Ahmed, R., 2019. Effects of Biochar on Uptake, Acquisition and Translocation of Silver Nanoparticles in Rice (Oryza Sativa L.) in Relation to Growth, Photosynthetic Traits and Nutrients Displacement. Environ. Pollut. 250, 728–736.

Abgottspon, F., Bigalke, M., Wilcke, W., 2015. Fast Colloidal and Dissolved Release of Trace Elements in a Carbonatic Soil after Experimental Flooding. Geoderma 259–260,

156–163.
Adams, N. W. H., Kramer, J. R., 1998. Reactivity of Ag ion with thiol ligands in the presence of iron sulfide. Environmental toxicology and chemistry 17(4), 625. doi.org/10.1002/etc.5620170415.
Al, P., Viraraghavan, T., 2005. Thallium: a review of public health and environmental concerns Environ. Int. 845 31 (4), 493–501.
Al-Najar, H., Kaschl, A., Schulz, R., Römheld, V., 2005. Effect of thallium fractions in the soil and pollution origins on tl uptake by hyperaccumulator plants: a key factor for the assessment of phytoextraction. Int. J. Phytoremediation 7, 55–67. https://doi.org/10.1080/16226510590915837.
Antić-Mladenović, S., Frohne, T., Kresović, M., Stärk, H.J., Savić, D., Ličina, V., Rinklebe, J., 2017. Redox-Controlled Release Dynamics of Thallium in Periodically Flooded Arable Soil. Chemosphere 178, 268–276.
Antoniadis, V., Levizou, E., Shaheen, S.M., Ok, Y.S., Sebastian, A., Baum, C., Prasad, M.N.V., Wenzel, W.W., Rinklebe, J., 2017. Trace Elements in the Soil-Plant Interface: Phytoavailability, Translocation, and Phytoremediation–A Review. Earth-Science Rev. 171, 621–645.
Antunes, E., Jacob, M.V., Brodie, G., Schneider, P.A., 2017. Silver Removal from Aqueous Solution by Biochar Produced from Biosolids via Microwave Pyrolysis. J. Environ. Manage. 203, 264–272.
Auvinen, H., Gagnon, V., Rousseau, D.P.L., Du Laing, G., 2017. Fate of Metallic Engineered Nanomaterials in Constructed Wetlands: Prospection and Future Research Perspectives. Rev. Environ. Sci. Bio/Technology 16, 207–222.
Awad, Y.M., Ok, Y.S., Abrigata, J., Beiyuan, J., Beckers, F., Tsang, D.C.W., Rinklebe, J., 2018. Pine Sawdust Biomass and Biochars at Different Pyrolysis Temperatures Change Soil Redox Processes. Sci. Total Environ. 625, 147–154.
Baalousha, M., 2009. Aggregation and disaggregation of iron oxide nanoparticles: Influence of particle concentration, pH and natural organic matter. Sci. Total Environ. 407, 2093–2101.
Beiyuan, J., Awad, Y.M., Beckers, F., Tsang, D.C.W., Ok, Y.S., Rinklebe, J., 2017. Mobility and Phytoavailability of As and Pb in a Contaminated Soil Using Pine Sawdust Biochar under Systematic Change of Redox Conditions. Chemosphere 178, 110–118.
Bell, R.A., Kramer, J.R., Compounds, Annual Review Structural Chemistry And Geochemistry Of Silver-Sulfur, 1999. Critical Review Vol, 18.
Biaduń, E., Sadowska, M., Ospina-Alvarez, N., Krasnodębska-Ostręga, B., 2016. Direct Speciation Analysis of Thallium Based on Solid Phase Extraction and Specific Retention of a Tl(III) Complex on Alumina Coated with Sodium Dodecyl Sulfate. Microchim. Acta 183, 177–183.
Blume, H.-P., Stahr, K., Leinweber, P., 2011. Bodenkundliches Praktikum. Berlin.
Casiot, C., Egal, M., Bruneel, O., Verma, N., Parmentier, M., Elbaz-Poulichet, F., 2011. Predominance of Aqueous Tl(I) Species in the River System Downstream from the Abandoned Carnoulès Mine (Southern France). Environ. Sci. Technol. 45, 2056–2064.
Chen, G., Zhang, Z., Zhang, Z., Zhang, R., 2018. Redox-Active Reactions in Denitrification Provided by Biochars Pyrolyzed at Different Temperatures. Sci. Total Environ. 615, 1547–1556.
Chen, Y.W., Deng, T.L., Filella, M., Belzile, N., 2003. Distribution and Early Diagenesis of Antimony Species in Sediments and Porewaters of Freshwater Lakes. Environ. Sci. Technol. 37, 1163–1168.
Couture, R.M., Charlet, L., Markelova, E., Madé, B., Parsons, C.T., 2015. On–Off Mobilization of Contaminants in Soils during Redox Oscillations. Environ. Sci. Technol. 49, 3015–3023. https://doi.org/10.1021/es5061879.
Dong, X., Ma, L.Q., Gress, J., Harris, W., Li, Y., 2014. Enhanced Cr(VI) Reduction and As (III) Oxidation in Ice Phase: Important Role of Dissolved Organic Matter from Biochar. J. Hazard. Mater. 267, 62–70.
de Jonge, L.W., Kjaergaard, C., Moldrup, P., 2004. Colloids and Colloid-Facilitated Transport of Contaminants in Soils. Vadose Zone J 3, 321–325.
El-Naggar, A., Shaheen, S.M., Ok, Y.S., Rinklebe, J., 2018. Biochar Affects the Dissolved and Colloidal Concentrations of Cd, Cu, Ni, and Zn and Their Phytoavailability and Potential Mobility in a Mining Soil under Dynamic Redox-Conditions. Sci. Total Environ. 624, 1059–1071.
El-Naggar, A., Shaheen, S.M., Ok, Y.S., Rinklebe, J., 2019. Release dynamics of As Co, and Mo in a biochar treated soil under pre-definite redox conditions. Science of the Total Environment 657, 686–695.
Eqani, S.A.M.A.S., Tanveer, Z.I., Qiaoqiao, C., Cincinelli, A., Saqib, Z., Mulla, S.I., Ali, N., Katsoyiannis, I.A., Shafqat, M.N., Shen, H., 2018. Occurrence of Selected Elements (Ti, Sr, Ba, V, Ga, Sn, Tl, and Sb) in Deposited Dust and Human Hair Samples: Implications for Human Health in Pakistan. Environ. Sci. Pollut. Res. 25, 12234–12245.
Evans, L. J., Barabash, S. J., 2010. Molybdenum, Silver, Thallium and Vanadium. In Trace Elements in Soils; pp 515–549.
Falke, A.M., Weber, J.H., 1994. Methylation of Inorganic Tin by Decayingspartina Alterniflora in Estuarine Water and by Estuarine Water. Appl. Organomet. Chem. 8, 351–359.
Frohne, T., Rinklebe, J., Diaz-Bone, R.A., Du Laing, G., 2011. Controlled Variation of Redox Conditions in a Floodplain Soil: Impact on Metal Mobilization and Biomethylation of Arsenic and Antimony. Geoderma 160 (3–4), 414–424.
Griffiths, P.R., 1992. The Handbook of Infrared and Raman Characteristic Frequencies of Organic Molecules. Vib. Spectrosc. 4, 121.
Guo, L., Warnken, K.W., Santschi, P.H., 2007. Retention Behavior of Dissolved Uranium during Ultrafiltration: Implications for Colloidal U in Surface Waters. Mar. Chem. 107, 156–166.
Hageman, P. L., Briggs, P. H., Desborough, G. A., Lamothe, P. J., Theodorakos, P. J., 2000. Synthetic precipitation leaching procedure (splp) leachate chemistry data for solid mine waste composite samples from southwestern new mexico, and leadville, colorado Open-File Report 00-33.
Han, Y.S., Seong, H.J., Chon, C.M., Park, J.H., Nam, I.H., Yoo, K., Ahn, J.S., 2018. Interaction of Sb(III) with Iron Sulfide under Anoxic Conditions: Similarities and Differences Compared to As(III) Interactions. Chemosphere 195, 762–770.
Hashimoto, Y., Takeuchi, S., Mitsunobu, S., Ok, Y.-S., 2017. Chemical Speciation of Silver (Ag) in Soils under Aerobic and Anaerobic Conditions: Ag Nanoparticles vs. Ionic Ag. J. Hazard. Mater. 322, 318–324.
Herath, I., Vithanage, M., Bundschuh, J., 2017. Antimony as a Global Dilemma: Geochemistry, Mobility, Fate and Transport. Environ. Pollut. 223, 545–559.
Hockmann, K., Lenz, M., Tandy, S., Nachtegaal, M., Janousch, M., Schulin, R., 2014. Release of Antimony from Contaminated Soil Induced by Redox Changes. J. Hazard. Mater. 275, 215–221.
Jacobson, A.R., McBride, M.B., Baveye, P., Steenhuis, T.S., 2005. Environmental Factors Determining the Trace-Level Sorption of Silver and Thallium to Soils. Sci. Total Environ. 345, 191–205.
Jia, Y., Xiao, T., Sun, J., Yang, F., Baveye, P.C., 2018. Microcolumn-Based Speciation Analysis of Thallium in Soil and Green Cabbage. Sci. Total Environ. 630, 146–153.
Joseph, S.D., Camps-Arbestain, M., Lin, Y., Munroe, P., Chia, C.H., Hook, J., Van Zwieten, L., Kimber, S., Cowie, A., Singh, B.P., et al., 2010. An Investigation into the Reactions of Biochar in Soil. Australian Journal of Soil Research; CSIRO PUBLISHING 48, 501–515.
Joseph, S, Graber, ER, Chia, C, Munroe, P, Donne, S, Thomas, T, Nielsen, S, Marjo, C, Rutlidge, H, Pan, GX, Li, L, Taylor, P, Rawal, A, Hook, J, 2013. Shifting paradigms: development of high-efficiency biochar fertilizers based on nano-structures and soluble components. Carbon Management 4 (3), 323–343. https://doi.org/10.4155/cmt.13.23.
Kabata-Pendias, A., 2011. Trace Elements in Soils and Plants. CRC Press.
Karbowska, B., Zembrzuski, W., Jakubowska, M., Wojtkowiak, T., Pasieczna, A., Lukaszewski, Z., 2014. Translocation and Mobility of Thallium from Zinc-Lead Ores. J. Geochemical Explor. 143, 127–135.
Kim, H.S., Kim, K.R., Yang, J.E., Owens, G., Nehls, T., Wessolek, G., Kim, K.H., 2016. Effect of Biochar on Reclaimed Tidal Land Soil Properties and Maize (Zea Mays L.) Response. Chemosphere 142, 153–159.
Klüpfel, L., Keiluweit, M., Kleber, M., Sander, M., 2014. Redox Properties of Plant Biomass-Derived Black Carbon (Biochar). Environ. Sci. Technol. 48 (10), 5601–5611.
Li, T., Jiang, J., Li, D., Wang, J., 2016. Solidifying effect of heavy metals in the vanadium deposit-polluted soil by iron-based solid agents. China Environ. Sci. 36 (7), 2108–2114.
Liu, L., Liu, G., Zhou, J., Wang, J., Jin, R., Wang, A., 2016. Improved Bioreduction of Nitrobenzene by Black Carbon/Biochar Derived from Crop Residues. RSC Adv. 6, 84388–84396.
Löv, Å., Cornelis, G., Larsbo, M., Persson, I., Sjöstedt, C., Gustafsson, J.P., Boye, K., Kleja, D.B., 2018. Particle- and Colloid-Facilitated Pb Transport in Four Historically Contaminated Soils - Speciation and Effect of Irrigation Intensity. Appl. Geochemistry 96, 327–338.
Melo, T.M., Bottlinger, M., Schulz, E., Leandro, W.M., Botelho de Oliveira, S., de Aguiar, Menezes, Filho, A., El-Naggar, A., Bolan, N., Wang, H., Ok, Y.S., et al., 2019. Management of Biosolids-Derived Hydrochar (Sewchar): Effect on Plant Germination, and Farmers' Acceptance. J. Environ. Manage. 237, 200–214.
Mitsunobu, S., Harada, T., Takahashi, Y., 2006. Comparison of Antimony Behavior with That of Arsenic under Various Soil Redox Conditions. Environ. Sci. Technol. 40, 7270–7276.
Mitsunobu, S., Takahashi, Y., Sakai, Y., Inumaru, K., 2009. Interaction of Synthetic Sulfate Green Rust with Antimony(V). Environ. Sci. Technol. 43, 318–323.
Nakamaru, Y.M., Altansuvd, J., 2014. Speciation and Bioavailability of Selenium and Antimony in Non-Flooded and Wetland Soils: A Review. Chemosphere 111, 366–371.
Nielsen, S.G., Wasylenki, L.E., Rehkämper, M., Peacock, C.L., Xue, Z., Moon, E.M., 2013. Towards an Understanding of Thallium Isotope Fractionation during Adsorption to Manganese Oxides. Geochim. Cosmochim. Acta 117, 252–265.
Palansooriya, K.N., Shaheen, S.M., Chen, S.S., Tsang, D.C.W., Hashimoto, Y., Hou, D., Bolan, N.B., Rinklebe, J., Yong, Y.S., 2020. Soil amendments for immobilization of potentially toxic elements in contaminated soils: A critical review. Environ Int. 134, 105046.
Peacock, C.L., Moon, E.M., 2012. Oxidative Scavenging of Thallium by Birnessite: Explanation for Thallium Enrichment and Stable Isotope Fractionation in Marine Ferromanganese Precipitates. Geochim. Cosmochim. Acta 84, 297–313.
Polack, R., Chen, Y.-W., Belzile, N., 2009. Behaviour of Sb(V) in the Presence of Dissolved Sulfide under Controlled Anoxic Aqueous Conditions. Chem. Geol. 262, 179–185.
Rader, S.T., Maier, R.M., Barton, M.D., Mazdab, F.K., 2019. Uptake and Fractionation of Thallium by Brassica Juncea in a Geogenic Thallium-Amended Substrate. Environ. Sci. Technol. 53, 2441–2449.
Ralph, L., Twiss, M.R., 2002. Comparative Toxicity of Thallium(I), Thallium(III), and Cadmium(II) to the Unicellular Alga Chlorella Isolated from Lake Erie. Bull. Environ. Contam. Toxicol. 68 (2), 261–268.
Rinklebe, J., Antoniadis, V., Shaheen, S.M., Rosche, O., Altermann, M., 2019. Health Risk Assessment of Potentially Toxic Elements in Soils along the Central Elbe River. Germany. Environ. Int. 126, 76–88.
Rinklebe, J., Knox, A. S., Paller, M., 2017. Trace elements in waterlogged soils and sediments. CRC Press; Taylor & Francis Group, New York, USA.
Rinklebe, J., Shaheen, S.M., Frohne, T., 2016a. Amendment of Biochar Reduces the Release of Toxic Elements under Dynamic Redox Conditions in a Contaminated Floodplain Soil. Chemosphere 142, 41–47.
Rinklebe, J., Shaheen, S.M., Yu, K., 2016b. Release of As, Ba, Cd, Cu, Pb, and Sr under pre-definite redox conditions in different rice paddy soils originating from the U.S.A. and Asia. Geoderma 270, 21–32.
Royer, R.A., Burgos, W.D., Fisher, A.S., Unz, R.F., Dempsey, B.A., 2002. Enhancement of biological reduction of hematite by electron shuttling and Fe(II) complexation.

Environ. Sci. Technol. 36, 1939–1946.
Ryan, J.N., Gschwend, P.M., 1994. Effect of solution chemistry on clay colloid release from an iron oxide-coated aquifer sand. Environ. Sci. Technol. 28, 1717–1726.
Settimio, L., McLaughlin, M.J., Kirby, J.K., Langdon, K.A., Lombi, E., Donner, E., Scheckel, K.G., 2014. Fate and Lability of Silver in Soils: Effect of Ageing. Environ. Pollut. 191, 151–157.
Shaheen, S.M., Niazi, N.K., Hassan, N.E.E., Bibi, I., Wang, H., Tsang, D.C.W., Ok, Y.S., Bolan, N., Rinklebe, J., 2019. Wood-Based Biochar for the Removal of Potentially Toxic Elements in Water and Wastewater: A Critical Review. Int. Mater. Rev. 64, 216–247.
Shaheen, S.M., Rinklebe, J., Frohne, T., White, J., DeLaune, R., 2016. Redox effects on release kinetics of arsenic, cadmium, cobalt, and vanadium in Wax Lake Deltaic soils. Chemosphere 150, 740–748.
Shaheen, S.M., Rinklebe, J., Frohne, T., White, J.R., DeLaune, R.D., 2014. Biogeochemical factors governing cobalt, nickel, selenium, and vanadium dynamics in periodically flooded Egyptian North Nile Delta rice soils. Soil Science Society of America Journal 78, 1065–1078.
Shaheen, S.M., Tsadilas, C.D., Rinklebe, J., 2013. A review of the distribution coefficients of trace elements in soils: Influence of sorption system, element characteristics, and soil colloidal properties. Adv. Colloid Interface Sci. 201–202, 43–56.
Sikora, F.J., Stevenson, F.J., 1988. Silver Complexation by Humic Substances: Conditional Stability Constants and Nature of Reactive Sites. Geoderma 42, 353–363.
Takeno, N., 2005. Atlas of Eh-pH diagrams. Geological survey of Japan open file report 419, 102.
Thompson, A., Chadwick, O.A., Boman, S., Chorover, J., 2006. Colloid mobilization during soil iron redox oscillations. Environ. Sci. Technol. 40, 5743–5749.
Trakal, L., Šigut, R., Šillerová, H., Faturíková, D., Komárek, M.K., 2014. Copper Removal from Aqueous Solution Using Biochar: Effect of Chemical Activation. Arab. J. Chem. 7, 43–52.
U.S. Environmental Protection Agency, 2007. Microwave assisted acid digestion of sediments, sludges, soils, and oils., vol, 3051A.
Van Koetsem, F., Woldetsadik, G.S., Folens, K., Rinklebe, J., Du Laing, G., 2018. Partitioning of Ag and CeO2 Nanoparticles versus Ag and Ce Ions in Soil Suspensions and Effect of Natural Organic Matter on CeO2 Nanoparticles Stability. Chemosphere 200, 471–480.
Vaněk, A., Grösslová, Z., Mihaljevič, M., Trubač, J., Ettler, V., Teper, L., Cabala, J., Rohovec, J., Zádorová, T., Penížek, V., et al., 2016. Isotopic Tracing of Thallium Contamination in Soils Affected by Emissions from Coal-Fired Power Plants. Environ. Sci. Technol. 50, 9864–9871.
Voegelin, A., Pfenninger, N., Petrikis, J., Majzlan, J., Plötze, M., Senn, A.C., Mangold, S., Steininger, R., Göttlicher, J., 2015. Thallium Speciation and Extractability in a Thallium- and Arsenic-Rich Soil Developed from Mineralized Carbonate Rock. Environ. Sci. Technol. 49, 5390–5398.
Wan, X., Tandy, S., Hockmann, K., Schulin, R., 2013. Changes in Sb Speciation with Waterlogging of Shooting Range Soils and Impacts on Plant Uptake. Environ. Pollut. 172, 53–60.
Wang, X.S., Chen, L.F., Li, F.Y., Chen, K.L., Wan, W.Y., Tang, Y.J., 2010. Removal of Cr (VI) with Wheat-Residue Derived Black Carbon: Reaction Mechanism and Adsorption Performance. J. Hazard. Mater. 175, 816–822.
Weber, F.A., Voegelin, A., Kaegi, R., Kretzschmar, R., 2009. Contaminant Mobilization by Metallic Copper and Metal Sulphide Colloids in Flooded Soil. Nat. Geosci. 2, 267–271.
Weishaar, J.L., Aiken, G.R., Bergamaschi, B.A., Fram, M.S., Fujii, R., Mopper, K., 2003. Evaluation of Specific Ultraviolet Absorbance as an Indicator of the Chemical Composition and Reactivity of Dissolved Organic Carbon. Environ. Sci. Technol. 37, 4702–4708.
Xiong, Y., 2007. Hydrothermal Thallium Mineralization up to 300 °C: A Thermodynamic Approach. Ore Geol. Rev. 32, 291–313.
Xu, X., Huang, H., Zhang, Y., Xu, Z., Cao, X., 2019. Biochar as Both Electron Donor and Electron Shuttle for the Reduction Transformation of Cr(VI) during Its Sorption. Environ. Pollut. 244, 423–430.
Yan, J., Lazouskaya, V., Jin, Y., 2016. Soil colloid release affected by dissolved organic matter and redox conditions. Vadose Zone J 15 (3). https://doi.org/10.2136/vzj2015.02.0026.
Yang, X., Tsibart, A., Nam, H., Hur, J., El-Naggar, A., Tack, F.M.G., Wang, C.H., Lee, Y.H., Tsang, D.C.W., Ok, Y.S., 2019. Effect of Gasification Biochar Application on Soil Quality: Trace Metal Behavior, Microbial Community, and Soil Dissolved Organic Matter. J. Hazard. Mater. 365, 684–694.
Yu, K., Rinklebe, J., 2011. Advancement in Soil Microcosm Apparatus for Biogeochemical Research. Ecol. Eng. 37 (12), 2071–2075.
Yuan, Y., Bolan, N., Prévoteau, A., Vithanage, M., Biswas, J.K., Wang, H., 2017. Applications of Biochar in Redox-Mediated Reactions. Bioresour. Technol. 246, 271–281.